ARMY RESEARCH LABORATORY

Scalable Implementation of Three-Dimensional Heterogeneous Media Subjected to Short Transient Impact Loads

by Rama R. Valisetty, Raju R. Namburu, and Peter W. Chung

ARL-TR-2351 September 2000

The findings in this report are not to be construed as an official Department of the Army position unless so designated by other authorized documents.

Citation of manufacturer's or trade names does not constitute an official endorsement or approval of the use thereof.

Destroy this report when it is no longer needed. Do not return it to the originator.

Army Research Laboratory
Aberdeen Proving Ground, MD 21005-5067

ARL-TR-2351 September 2000

Scalable Implementation of Three-Dimensional Heterogeneous Media Subjected to Short Transient Impact Loads

Rama R. Valisetty, Raju R. Namburu, and Peter W. Chung
Computational and Information Sciences Directorate, ARL

Abstract

This report is concerned with developing and implementing scalable algorithmic approaches for solving coupled micro and macro structural applications based on the asymptotic expansion homogenization (AEH) method. AEH for nonlinear and short transient loading applications is computationally demanding and cannot be addressed on serial computers. Hence, the emphasis of the present investigation is to develop and implement consistent AEH numerical formulations on scalable computers to address elasto-plastic material response of structures subjected to short transient loading. A second order, accurate velocity-based, explicit time integration method, in conjunction with the AEH method on scalable computing architectures, is implemented using message-passing interface (MPI). Two different scalable implementation approaches are discussed, and the scalability of the computational approach is demonstrated.

Table of Contents

INTENTIONALLY LEFT BLANK

List of Figures

INTENTIONALLY LEFT BLANK.

List of Tables

INTENTIONALLY LEFT BLANK.

1. Introduction

Many practical military structural analysis problems are concerned with heterogeneous media subjected to short impact or transient loading. For these heterogeneous media applications, the challenges include accurately assessing various failure modes at the micro-mechanics level, expressing constitutive model with effective material properties at the macro-mechanics level, and understanding the relationship between micro and macro levels. The effective material properties can be obtained either by using mathematical homogenization theory [1–5] or its engineering counterpart [6–10]. For short transient impact loading condition, a detailed knowledge of the material flow in and around material micro structural constituents, and material interfaces is necessary. This flow is three-dimensional, transient, nonlinear, and the controlling global loads are of short duration impact. Classical theories such as rule of mixtures that are based on constant stress or strain assumption leads to an aggregation of the response in the micro-structural details and thus are of limited use.

Recent advances in mathematically rigorous asymptotic expansion homogenization (AEH) methods enable the coupling of micro and macro approaches for both linear and nonlinear structural applications [11–15]. Most recently, Chung et al. [16] demonstrated the applicability of AEH method for heterogeneous media subjected to short transient loading by employing explicit dynamics finite element formulations in conjunction with elasto-plastic material response. Using the AEH approach, the micro-level variables were expressed as direct functions of the macro-level variables in a strict, mathematically seamless approach. Their work [16] was especially suitable for conducting explicit transient elasto-plastic analysis of heterogeneous materials. An updated Lagrangian scheme for small strains and small rotations is employed to account for large displacements, strains, and rotations over many time steps. At each time, the equilibrium solution from the previous time step is used to update the position of the nodal coordinates such that the next simulation computes its solution based on the new equilibrium configuration. Updating the mesh at every solution interval allows for the subsequent interval to employ the last equilibrium state as its reference state. Since an explicit time integration scheme takes quite a large number of time steps and the macro- and micro-level

computations are to be performed at each time step and for each global finite element, the attendant micro and macro computations can take much longer times for solution. Scalable computational approaches are needed to explore these computationally intensive methods.

General purpose explicit dynamics codes like PARADYN [17] and PRONTO3D [18] demonstrated large scale analyses on a variety of scalable computing platforms using message-passing interface (MPI) libraries and domain decomposition. Macro-mechanics implementation of the proposed method on scalable computers is similar to these general purpose explicit dynamics codes. The investigation of Chung et al. [16] considers the dynamic equation of motion discretized according to a second order accurate scheme as presented in Namburu [19]. In addition to macro-mechanics explicit formulations, the proposed AEH formulation requires coupling, and solving the local micro-structural response in terms of the global macro structural response. One strategy that was explored extensively was based on using a global domain decomposition scheme for spreading the global finite element computations across a grid of processing nodes, and then using a separate set of processors for the micro-element computations. In a later extension of this approach, the global processors that are finished with their part of computations ahead of other processors were put to use in helping with the micro-element computations in other domains. Scalability of the approach is demonstrated for a Taylor impact problem. The results obtained on an IBM-SP2 showed consistent scaling with 2, 4, 8, 16, 32, and 64 processor computations.

The outline of this report is as follows. Section 2 introduces the fundamental ideas of the mathematical and numerical formulations of the asymptotic expansion homogenization method. Section 3 discusses the algorithmic issues and implementation of the AEH method on scalable computers. Scalability of the approach is discussed in section 4.

2. Mathematical Formulations

2.1 Governing Equations. Assume a three-dimensional body Ω is an assembly of periodic structures containing different material as shown in Figure 1. Typically, the unit cell is very

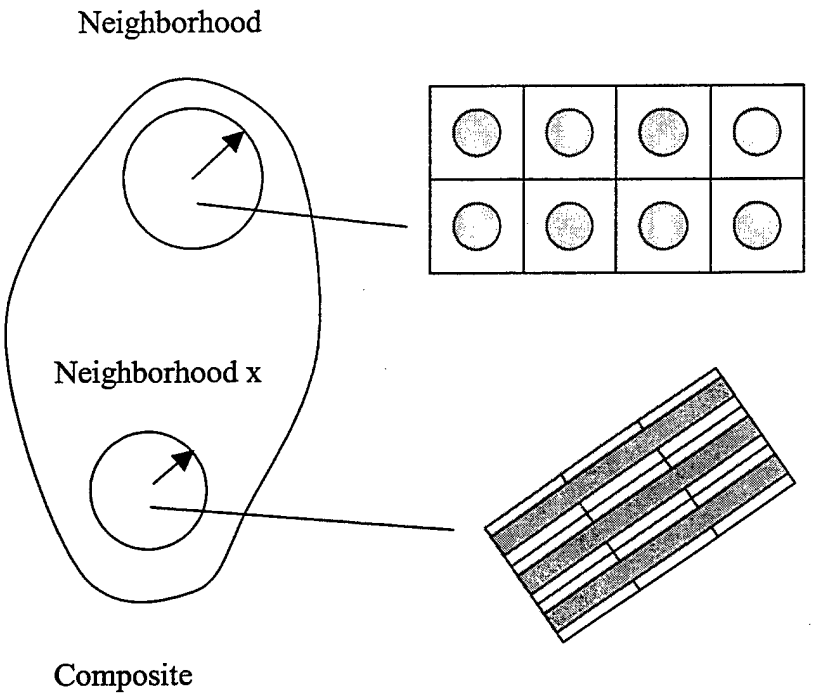

Figure 1. Macro-Micro Analyses' Neighborhoods.

small, of order ε (where ε is a small positive number) compared to the dimensions of the problem domain. Structural response quantities such as displacements, velocities, stresses, and strains are assumed to have slow variations (macroscopic) from point to point as well as fast (microscopic) variations within a small neighborhood ε of a given point x. Let Y be a (periodic) representative part of Ω. Here we distinguish two scales: the macroscopic scale ($x \in \Omega$) and microscopic scale ($y \in \Omega$). Lagrangian representation of conservation of mass and momentum equations are used in this study. The conservation of mass is used to calculate the current density from the initial density. The momentum equation, the kinematic relations, and the constitutive model are represented by

$$\rho^{\varepsilon} \dot{v}_i^{\varepsilon} - \sigma_{ji,j}^{\varepsilon} = f_i, \tag{1}$$

$$\dot{e}_{ij}^{\varepsilon} = \frac{1}{2}(v_{i,j}^{\varepsilon} + v_{j,i}^{\varepsilon}), \tag{2}$$

and

$$\sigma_{ij}^{\varepsilon} = S_{ij}(\dot{e}_{ij}^{\varepsilon}, E), \tag{3}$$

where ρ is the density, f_i is the body force vector, E is the internal energy, the superscript ε denotes micro/macro continuum solutions, v_i is the velocity vector, σ_{ij} is the stress tensor, and e_{ij} is the strain tensor. The initial conditions in the domain Ω^{ε}, boundary conditions on the surface of the domain Γ ($\Gamma_1 \cup \Gamma_2$) are given by

$$u_i^{\varepsilon}(t=0) = u_{o_i}^{\varepsilon}, \tag{4}$$

$$v_i^{\varepsilon}(t=0) = v_{o_i}^{\varepsilon}, \tag{5}$$

$$u_i^{\varepsilon} = u_i^{o\varepsilon} \quad \text{on } \partial\Gamma_1, \tag{6}$$

and

$$\sigma_{ji}^{\varepsilon} n_i = T_i \quad \text{on } \partial\Gamma_2, \tag{7}$$

where u_i is the displacement vector and n_i is a surface normal.

2.2 Time Integration. Second order accurate Lax-Wendroff based explicit time integration procedure [20] is employed for the conservation equation or equation of motion. In this approach, the dependent variable velocity is first discretized in time using second order Taylor series expansion.

$$v_i^{\varepsilon^{n+1}} = v_i^{\varepsilon^n} + \Delta t \dot{v}_i^{\varepsilon^{n+1/2}}. \tag{8}$$

Taking appropriate time derivatives of equation (1) and substituting for the velocity and acceleration gives

$$\rho v_i^{\varepsilon^{n+1}} - \rho v_i^{\varepsilon^n} = \sigma_{ji,j}^{\varepsilon^{n+1/2}} + \rho f_i^{n+1/2}. \tag{9}$$

The stress increment is related to a strain increment through an appropriate constitutive equation. The elasto-plastic constitutive equation at midpoint time increment is defined by

$$\sigma_{ij}^{\varepsilon^{n+1/2}} = M_{ijkl}(\sigma_{ij}^{\varepsilon^{n-1/2}} + C_{klmn}\dot{\varepsilon}_{mn}^{\varepsilon^{n-1/2}} \Delta t^{n+1/2}). \tag{10}$$

Stresses and strain rates at midpoint time can be evaluated using the predicted displacements as shown:

$$u_i^{\varepsilon^{n+1/2}} = u_i^{\varepsilon^n} + \frac{\Delta t}{2} v_i^{\varepsilon^{n+1/2}}. \tag{11}$$

2.3 Asymptotic Expansion and Elasto-plastic Constitutive Equations. The homogenization method is based on the asymptotic expansion of the primary variables together with a unit cell approach for a heterogeneous structure. Assume a three-dimensional body Ω is an assembly of periodic structures (1). Typically, the unit cell is very small, of order ε (ε is a small positive number) compared to the dimensions of the problem domain. Typically, two-scale asymptotic expansion can be employed to approximate the displacement, velocity, strain, or stress fields.

$$u_i^{\varepsilon}(x,y) = u_{o_i}(x,y) + \varepsilon u_{1_i}(x,y) + \varepsilon^2 u_{2_i}(x,y) + \cdots, \tag{12}$$

$$v_i^{\varepsilon}(x,y) = v_{o_i}(x,y) + \varepsilon v_{1_i}(x,y) + \varepsilon^2 v_{2_i}(x,y) + \cdots, \tag{13}$$

$$e_i^{\varepsilon}(x,y) = e_{o_i}(x,y) + \varepsilon e_{1_i}(x,y) + \varepsilon^2 e_{2_i}(x,y) + \cdots, \tag{14}$$

and

$$\sigma_i^{\varepsilon}(x,y) = \sigma_{o_i}(x,y) + \varepsilon \sigma_{1_i}(x,y) + \varepsilon^2 \sigma_{2_i}(x,y) + \cdots, \tag{15}$$

where $u_i^\varepsilon(x,y)$, $v_i^\varepsilon(x,y)$, $e_i^\varepsilon(x,y)$, and $\sigma_i^\varepsilon(x,y)$ are Y-periodic functions.

The AEH approach for nonlinear applications is based on the instantaneously linearized assumption for the constitutive model, Terada and Kikuchi [12]. The fundamental assumption of the AEH approach, therefore, is that the true solution in the ε space is decomposed into a macro space x and a micro space y. The basic assumption here is that multiple scales exist only in the spatial variables and that no such scaling exists for the time variable. Further reading in space *and* time asymptotic expansion approaches can be found in Benoussan et al. [4]. The general approach to heterogeneous problems is to separate and draw clear distinction between the micro- and macro-level equilibrium equations regardless, per the earlier linearized assumption, of material nonlinearity. This is accomplished by asymptotically expanding the primary variables where the asymptotic scale is approximated to the second order.

$$v_i^\varepsilon(x,y) = v_{o_i}(x,y) + \varepsilon v_{1_i}(x,y) + \varepsilon^2 v_{2_i}(x,y) + \cdots. \tag{16}$$

Spatial gradients in ε-space are taken with respect to the x-coordinate system. The corresponding gradient for Y-periodic functions (where micro and macro are now distinguishable) is given by the chain rule where the scaling is defined by $y = x/\varepsilon$, and hence for any Y-periodic function ϕ, the earlier gradients are replaced by

$$\frac{d\phi}{dx_i} = \frac{\partial\phi}{\partial x_i} + \frac{1}{\varepsilon}\frac{\partial\phi}{\partial y_i}. \tag{17}$$

Then, using equation (1) in equation (7) while considering equation (2) gives the rate of strain tensor defined by

$$\dot{\varepsilon}_{ij}^\varepsilon = [e_{ij}^x(v_o) + e_{ij}^y(v_1)] + \varepsilon[e_{ij}^x(v_1) + e_{ij}^y(v_2)] + \cdots, \tag{18}$$

where the symmetrized gradient tensors, $e^x{}_{ij}$ and $e^y{}_{ij}$ are defined by

$$e_{ij}^{x}(\phi) = \frac{1}{2}\left(\frac{\partial \phi_i}{\partial x_j} + \frac{\partial \phi_j}{\partial x_i}\right) \tag{19}$$

and

$$e_{ij}^{y}(\phi) = \frac{1}{2}\left(\frac{\partial \phi_i}{\partial y_j} + \frac{\partial \phi_j}{\partial y_i}\right). \tag{20}$$

The relevant expressions for gradients and velocities are first substituted into the governing equations of motion. Next, the micro and macro equations are identified by selecting the appropriate coefficients to the scaling factors ε which must each be identically zero. Substituting the asymptotically expanded velocities, equation (1), in the strain rate, equation (3), and then using the constitutive equation, equation (16), in the equations of motion, equation (15), yields a set of equations dependent on powers of ε. To satisfy the equations of motion, each term associated with each of the powers of ε must approach zero identically. This leads to a set of equations associated with the microscopic and macroscopic equations of motion. The first equation, associated with the powers of ε^{-2} is given by

$$\varepsilon^{-2}: \quad \frac{\partial}{\partial y_j} C_{ijkl}^{*} \frac{\partial v_{o_k}^{n-1}}{\partial y_l} = 0, \tag{21}$$

where $C_{ijkl}^{*} = M_{ijpq} C_{pqkl}$. Equation (21) states that $v_{o_k}^{n-1}$ is a function only of x. Hence, derivatives of y are zero. Using this inference, the equation associated with the powers of ε^{-1} is derived as

$$\varepsilon^{-1}: \quad \frac{\partial}{\partial y_j} C_{ijkl}^{*} \frac{\partial v_{o_k}^{n-1}}{\partial x_l} + \frac{\partial}{\partial y_j} C_{ijkl}^{*} \frac{\partial v_{1_k}^{n-1}}{\partial y_l} = -\frac{1}{\Delta t} \frac{\partial}{\partial y_j} (M_{ijkl} \sigma_{kl}^{n-1/2}). \tag{22}$$

Equation (22) relates the perturbative velocity field, v_1, to the macroscopic velocity field, v_o. An equation relating these two quantities become the important micro-macro equation, providing

the direct link to relate microscopic to the macroscopic velocities. Such an equation is also called the *localization* equation due to its features. The localization equation is given by

$$v_{1_i}^{n-1} = -\chi_i^{mn^1} \frac{\partial v_{o_m}^{n-1}}{\partial x_n} - \frac{1}{\Delta t} \chi_i^2 + \tilde{v}_{1_i}(x), \tag{23}$$

where $\tilde{v}_{1_i}$ is a constant of integration, and the corrector functions (sometimes referred to as the so-called characteristic functions) are the solutions to the equations

$$\frac{\partial}{\partial y_j} C_{ijkl}^* \frac{\partial \chi_k^{mn^1}}{\partial y_1} = \frac{\partial}{\partial y_j} C_{ijmn}^*, \tag{24}$$

and

$$\frac{\partial}{\partial y_j} C_{ijkl}^* \frac{\partial \chi_k^2}{\partial y_1} = \frac{\partial}{\partial y_j} M_{ijkl} \sigma_{kl}^{\varepsilon^{n-1/2}}. \tag{25}$$

Equations (24) and (25) are the corrections which account for the shape of the interface separating various phases and the time-dependent plastic softening effect due to material nonlinearities, respectively. Clearly, for a homogeneous problem, both correctors are identically zero. In the event where no plastic yielding occurs, the problem degenerates to a transient elastic problem. These equations arising from equation (22) constitute the microscale problem.

Finally, the equation associated with the powers of ε^0 is written as

$$\begin{aligned} \varepsilon^0: \quad & \frac{\partial}{\partial x_j} C_{ijkl}^* \frac{\partial v_{o_k}^{n-1}}{\partial x_l} + \frac{\partial}{\partial x_j} C_{ijkl}^* \frac{\partial v_{1_k}^{n-1}}{\partial y_l} + \frac{\partial}{\partial y_j} C_{ijkl}^* \frac{\partial v_{o_k}^{n-1}}{\partial x_l} + \frac{\partial}{\partial y_j} C_{ijkl}^* \frac{\partial v_{2_k}^{n-1}}{\partial y_l} \\ & = \frac{\rho}{\Delta t^2} \Delta v_{o_i}^{n+1} - \frac{1}{\Delta t} \frac{\partial}{\partial x_j} M_{ijkl} \sigma_{kl}^{\epsilon^{n-1/2}} - \frac{\rho}{\Delta t} f_i^{n+1/2}. \end{aligned} \tag{26}$$

Much like equation (22) provided the basis for the micro-scale problem, equation (26) provides the basis for the macro-scale problem. By taking the volume average of equation (26), substituting for v_1 using the localization equation (23) and noting the periodicity, the final governing equation of motion is given by

$$\langle\rho\rangle\Delta v_{o_i}^{n+1} = \Delta t \frac{\partial}{\partial x_j}\left\langle\sigma_{ij}^{n+1/2} - \sigma_{ij}^{c}\right\rangle + \Delta t\langle\rho\rangle f_i^{n+1/2}, \tag{27}$$

where the "corrector stress," σ_{ij}^{c}, is defined by

$$\sigma_{ij}^{c} = C_{ijkl}^{*}\left(\frac{\partial\chi_k^2}{\partial y_l} + \frac{\partial\chi_k^{mn^1}}{\partial y_l}\frac{\partial v_{o_m}^{n=1}}{\partial x_n}\Delta t\right) \tag{28}$$

and where quantities in brackets denote

$$\langle(\ )\rangle = \frac{1}{V}\int_Y (\ )dY\,. \tag{29}$$

It is of interest to note that equation (27), for heterogeneous conditions, is similar in form to equation (6), the homogeneous equation, making the integration of a micromechanical problem into a macro analysis tractable and straightforward.

2.4 Constitutive Equation: Elasto-plastic. The stress tensor is split into two parts. The first part, S_{ij}, is deviatoric stress, which is related to material strength, and the second part is pressure P. To simplify notation, the superscript ε has been omitted.

$$\sigma_{ij} = -\delta_{ij}P + S_{ij}, \tag{30}$$

and

$$\frac{1}{3}\sigma_{ii} = -P. \tag{31}$$

The first term in equation (30) accounts for volumetric changes and is typically evaluated from equations of state in explicit dynamics. The second term, the stress deviator, is related to the deformation of the material and is defined by a constitutive model, and in particular, the time rate of change of the deviator is evaluated from the strain rates.

$$S_{ij} = 2G\varepsilon_{ij} + \Delta_{ij}, \tag{32}$$

where G is the shear modulus and Δ_{ij} is the correction for rigid body rotation.

An isotropic hardening model with a rate-dependent Von Mises yield condition is employed in the present analysis. A consistency condition ensures that the stress state remains on the yield surface at the start and end of a time-step. Such a condition is given by

$$R^{n+1}Q_{ij} = S_{ij}^{n+1}. \tag{33}$$

The variable R is the rate-dependent radius of the yield surface or the apparent yield stress, Q_{ij} is the vector specifying the normal direction to the yield surface, and S_{ij} is the deviatoric component of the stress. The stresses are understood to be the co-rotated second-order tensor according to the Jaumann definition of the co-rotational derivative. The Jaumann derivative of the Cauchy stress, $\dot{\sigma}_{ij}^{J}$ is related to the material time derivative, $\dot{\sigma}_{ij}$ by

$$\dot{\sigma}_{ij}^{J} = \dot{\sigma}_{ij} + \sigma_{ik}\omega_{kj} + \omega_{ik}\sigma_{kj}, \tag{34}$$

where ω_{kj} is the rotation tensor, the standard skew-symmetric component of the velocity gradient. The radius of the yield surface is defined by

$$R = \sigma_Y^o \left[1 + \left(\frac{\bar{e}}{D} \right)^{\frac{1}{p}} \right] + H' \bar{\varepsilon}^{\,p}, \tag{35}$$

where σ_Y^o is the static yield stress of the material and D and p are the so-called fluidity parameters. H' is the hardening parameter, and $\bar{\varepsilon}^{\,p}$ is the effective plastic strain. The effective rate of deformation, $\bar{\varepsilon}$ is defined by

$$\bar{e} = \sqrt{\frac{2}{3} \dot{e}_{ij} \dot{e}_{ij}}, \tag{36}$$

where e_{ij} is the deviatoric component of the total strain ε_{ij}. The normality condition, specified by the normal vector Q_{ij}, is given by

$$Q_{ij} = \frac{S_{ij}}{\sqrt{S_{mn} S_{mn}}}. \tag{37}$$

For a homogeneous material (which is applicable in the present derivation since the constitutive equations are applied at the micro level where the material is homogeneous within each phase) the incremental relationships for the apparent yield stress and the deviatoric stress are defined as

$$R^{n+1} = R^n + \frac{2}{3} H' \Delta\lambda, \tag{38}$$

and

$$S_{ij}^{n+1} = S_{ij}^{n+1^T} - 2G\Delta\lambda Q_{ij}, \tag{39}$$

where $S_{ij}^{n+1^T}$ is the deviatoric trial stress, $\Delta\lambda$ is a scalar quantity representing the magnitude of the radial return correction due to plastic yielding, and G is the elastic shear modulus. The deviatoric trial stress is defined by

$$S_{ij}^{n+1^T} = S_{ij}^n + C_{ijkl}\dot{e}_{kl}^n \Delta t \ , \tag{40}$$

where C_{ijkl} is the tensor containing elastic properties.

Finally, substituting equations (41) and (39) into equation (33) and solving for the radial return correction parameter gives

$$\Delta\lambda = \frac{3/2}{(3G + H')}\left(\sqrt{\frac{3}{2}S_{ij}^{n+1^T}S_{ij}^{n+1^T}} - R_n\right). \tag{41}$$

Using equation (40) in equation (41) and employing the standard assumption that a material is elastic in its dilatational behavior and plastic only in shear gives the total stress increment in equation (16). The constitutive equation (16) can now be employed in the derivation of the micro and macro governing equations.

3. Computational and Implementation Issues

3.1 Macro Finite Element Equations. Finally, in the absence of damping, the discretized equations are given in matrix form by

$$\boldsymbol{M}\Delta\boldsymbol{v}^{n+1} = \boldsymbol{F}_1^{n+1/2} + \boldsymbol{F}_2^{n+1/2} + \boldsymbol{F}_3^{n+1/2}, \tag{42}$$

where the displacements are given by

$$u_i^{n+1} = u_i^n + \Delta t\left[(1-\gamma)v_i^n + \gamma v_i^{n+1}\right] \tag{43}$$

and

$$\boldsymbol{M} = \int_{\Omega_e} N_\alpha \rho N_\beta d\Omega_e\,, \tag{44}$$

$$\boldsymbol{F}_1^{n+1/2} = \Delta t \int_{\Omega_e} N_{\alpha i} \left\{\sigma^{*^{n+1/2}}\right\} d\Omega_e\,, \tag{45}$$

$$\boldsymbol{F}_2^{n+1/2} = -\Delta t \int_{\partial\Omega_e} N_\alpha \left\{\sigma^{*^{n+1/2}} \cdot \hat{\boldsymbol{n}}\right\} d\Omega_e\,, \tag{46}$$

$$\boldsymbol{F}_3^{n+1/2} = \Delta t \int_{\Omega_e} N_\alpha \rho \boldsymbol{f}^{n+1/2} d\Omega_e\,, \tag{47}$$

$$\Delta \boldsymbol{v}^{n+1} = \boldsymbol{v}^{n+1} - \boldsymbol{v}^n\,, \text{ and} \tag{48}$$

$$\boldsymbol{f}^{n+1/2} = \frac{1}{2}(\boldsymbol{f}^{n+1} + \boldsymbol{f}^n)\,. \tag{49}$$

The subscript e denotes element quantities, and γ is a free parameter. The volume averaging brackets are implied for densities and stresses. The stresses are defined by

$$\sigma_{ij}^{*^{n+1/2}} = \sigma_{ij}^{n+1/2} - \sigma_{ij}^c\,, \tag{50}$$

where σ_{ij}^c is the stress corrector. The mass matrix $\boldsymbol{M}$ in equation (44) is lumped for the present explicit formulation. The vectors $\boldsymbol{F}_1$, $\boldsymbol{F}_2$, and $\boldsymbol{F}_3$ are due to internal forces, boundary tractions, and external loads, respectively.

3.2 Micro Finite Element Equations. In order to compute each term in equation (44), the effective microscopic quantities for density and stresses must first be homogenized over the representative unit cell associated with that macro-level finite element. Despite the explicit formulation in the macro-level which avoids the solution of a set of equations, the micro-level equations require an iterative implicit solution of a sparse equation set. This is less computation than required in the quasi-static approach which requires solutions of both the micro-level equations *and* the macro-level equations. The present method avoids the solution of macro-level equations.

The discretized forms of the micro-level equations are given by

$$\boldsymbol{K}\chi^1 = \boldsymbol{F}_1^{micro}, \tag{51}$$

and

$$\boldsymbol{K}\chi^2 = \boldsymbol{F}_2^{micro}, \tag{52}$$

where

$$\boldsymbol{K} = \int_Y N_{\alpha,i}[C^*]N_{\beta,i}dY, \tag{53}$$

$$\boldsymbol{F}_1^{micro} = \int_Y N_{\alpha,i}[C^*]dY, \tag{54}$$

and

$$\boldsymbol{F}_2^{micro} = \int_Y N_{\alpha,i}[M]\{\sigma^{n-1/2}\}dY. \tag{55}$$

Equation (51) possesses six right-hand side vectors corresponding with the six columns in $[C^*]$ while equation (52) possesses one right-hand side. Thus, for each macro-level element, seven sets of equations must be solved. Since the stiffness matrix is the same in each equation, a solver which can re-employ its factored stiffness matrix is warranted. The micro-level stresses

are computed from equation (16), implying that every micro-level element stress must be stored between successive time steps, which are then averaged to give the macro-level stresses via the volume averaging operator.

For true generality, the nonlinear equations (51) and (52) must be solved for each macro-level element because of micro-level stress variations which may occur. In light of the added computation required in multiscale analyses, the computational complexity, a subjective measure of the computation time, increases substantially for a micro or macro problem compared to a simple single-length scale macro problem.

3.3 Scalable Implementation. This section discusses scalable implementation aspects of explicit macro finite element formulations and implicit micro finite element formulations. To enhance the scalable speed-up, two different micro-element implementation strategies were discussed.

3.3.1 Scalable Approach for Macro Finite Element Method. The macro approach uses the self-starting velocity based explicit time integration algorithm of reference [20] in conjunction with the elasto-plastic constitutive relations and large deformation as shown in Figure 2.

Note that the explicit time integration scheme does not involve any system of equations to be solved. Similar to other large deformation, explicit time integration codes, the present approach uses one-point integration to evaluate the element integrals. First, the finite element mesh is partitioned into subdomains using the domain decomposition approach based graph theory and in particular METIS software of reference [21]. This approach gives optimum mesh partitioning based on edge cuts. The number of subdomains partitioned is equal to the number of processors being used. Next, the MPI is used to communicate information between the processors. Figure 3 depicts the process.

Given the following equations of motion, $\rho \ddot{u} + \sigma_{ij,j} = f_e$,
subjected to the following boundary conditions, $u_i = U_i$ on Γ_{i1} and
$\sigma_{ij} = Ti$ on Γ_{i2},
and the initial conditions, $u_i(t=0) = u^0_i$ and
$\dot{u}_i(t=0) = \dot{u}^0_i$,

with ρ = density, $\ddot{u}$ = acceleration, σ_{ij} = internal forces, and f_e = external forces; then the numerical algorithm begins with an assumption for the time integration.

An example of a scheme based on the central difference is given below. The solution begins with the initial conditions for the displacements and velocities at time step n = 0. It progresses in the following substeps for each Δt_n:

Step 1: Predictor step:
$$u^{n+1/2} = u^n + \frac{\Delta t}{2}\dot{u}^n.$$

Step 2: Velocity increment solution step:
$$M\Delta U^{n+1} = F_1^{n+1/2} + F_2^{n+1/2} + F_3^{n+1/2}.$$

Step 3: Corrector step:
$$u^{n+1} = u^n + \frac{\Delta t}{2}[\dot{u}^{n+1} + \dot{u}^n],$$
where the element integrals in the above are given as
$$M = \int_{\Omega_e} N_\alpha \rho N_\beta d\Omega_e,$$
$$F_1 = \Delta t \int_{\Omega_e} N_{\alpha,i} \left\{\sigma^{*n+1/2}\right\} d\Omega_e,$$
$$F_3 = \Delta t \int_{\Omega_e} N_\alpha \rho f^{n+1/2} d\Omega_e, \text{ and}$$
$$F_2 = -\Delta t \int_{\partial\Omega_e} N_\alpha \left\{\sigma^{*n+1/2} \cdot \hat{n}\right\} d\Omega_e.$$

Step 4: Continue the corrector step to update the velocities, displacements, coordinates, time, and stresses:
$$\dot{u}^{n+\frac{1}{2}} = \dot{u}^{n-\frac{1}{2}} + \ddot{u}^n \Delta t^n,$$
$$\Delta u^{n+1} = \dot{u}^{n+1} - \dot{u}^n,$$
$$x^{n+1} = x^n + \dot{u}^{n+\frac{1}{2}} \Delta t^{n+\frac{1}{2}},$$
$$\Delta t^{n+\frac{1}{2}} = \frac{\Delta t^n + \Delta t^{n+1}}{2}, \text{ and}$$
$$\sigma_{ij}^{*n+1/2} = \sigma_{ij}^{n+1/2} - \sigma_{ij}^c.$$

Step 5: Check Δt for Courant stability criteria and continue Steps 1 through 4 until specified time limit.

Figure 2. A typical Algorithm for the Explicit Integration of Equations of Motion.

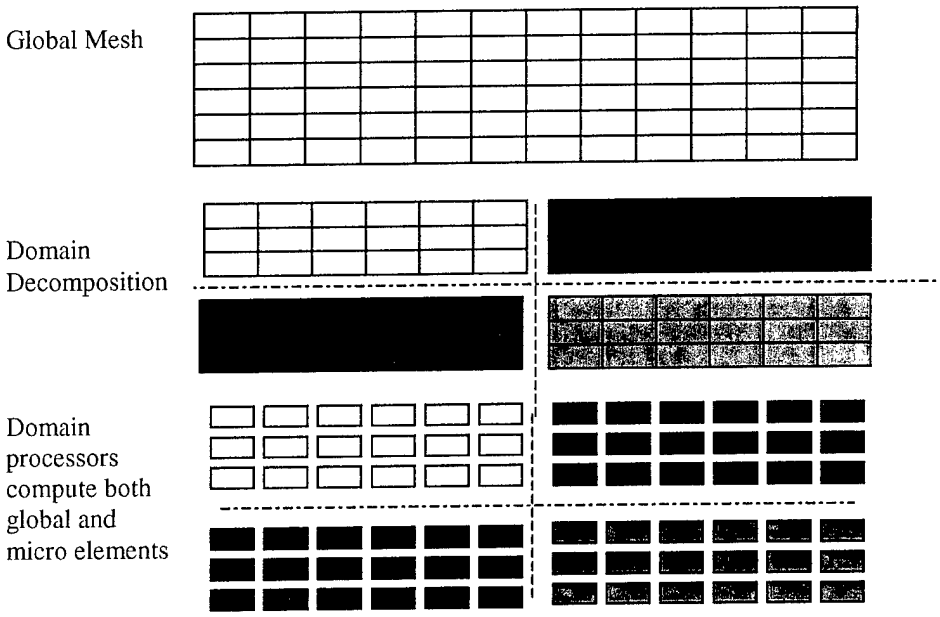

Figure 3. Strategy 1 Showing Domain Processors Computing Both Micro and Global Elements.

3.3.2 Scalable Approaches for Micro Finite Element Method. As opposed to the macro finite element method which uses the explicit time integration approach, the micro finite element approach involves solving systems of equations. Each macro element carries with it a micro-element model representing its micro-structural detail. In a traditional finite element, the material constitutive behavior is sampled at its integration points. In a similar manner, the constitutive behavior of a macro-element in the current program is obtained by solving the respective micro-element equations, at each time step. The micro-element solutions include the micro-element stresses, accumulated plastic strain, and the elastic and plastic material properties. Since AEH theory assures that these equations can be expressed solely in terms of the macro element response variables, the micro-element model computations are independent across the macro elements and across the different decomposition domains. That is, different strategies can be used to implement micro-element computations on scalable computers. In this study, two strategies are explored, and the issues of implementation and efficiency of the implementation are discussed next.

The two parallel implementation strategies are discussed.

(1) Domain decomposition for macro elements with the domain processors also doing the computations of their respective micro-structural models (Figure 3).

(2) Domain decomposition for macro elements with each domain processor assigned with helper processors for doing micro-structural model computations (Figure 4).

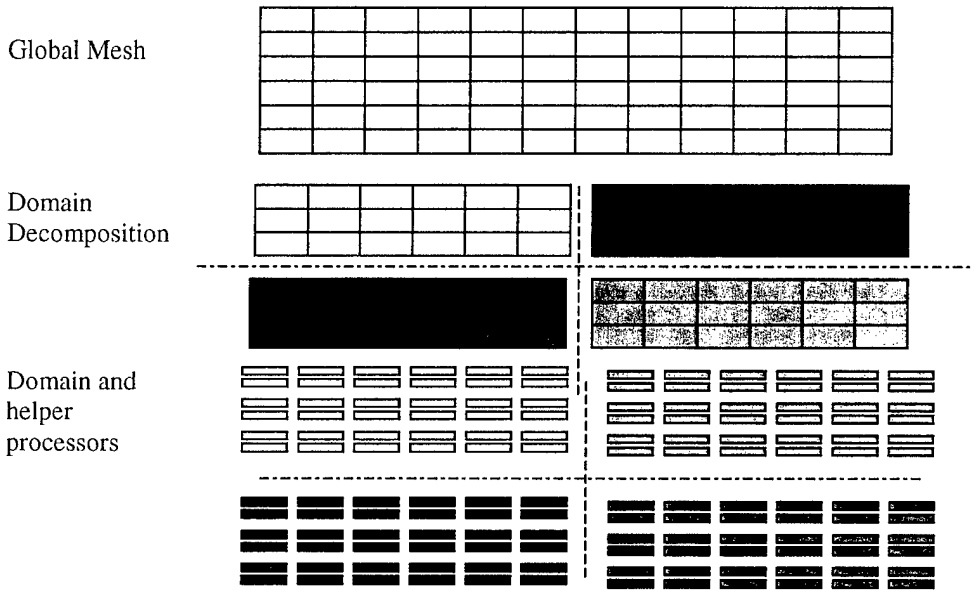

Figure 4. Strategy 2 Showing Helper Processors Computing Only Micro-elements and Global Processors Computing Both Global and Micro-elements.

Figures 5 and 6 present the program flow for these two strategies. In the first strategy, the computations begin with the gathering of the following information: the macro-element coordinates, the micro-element coordinates, mechanical properties, plasticity properties, average macro-element stresses, detailed micro-element stresses, average macro-element plastic strains, detailed micro-element plastic strains, and the current velocity increments at the macro-element nodes.

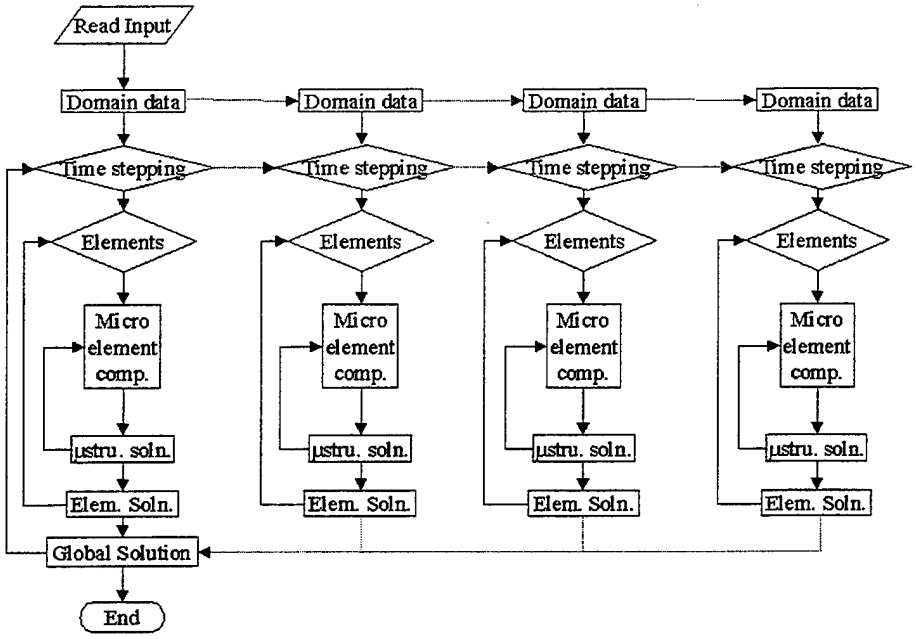

Figure 5. Program Flow for Strategy 1 Without Helper Processors.

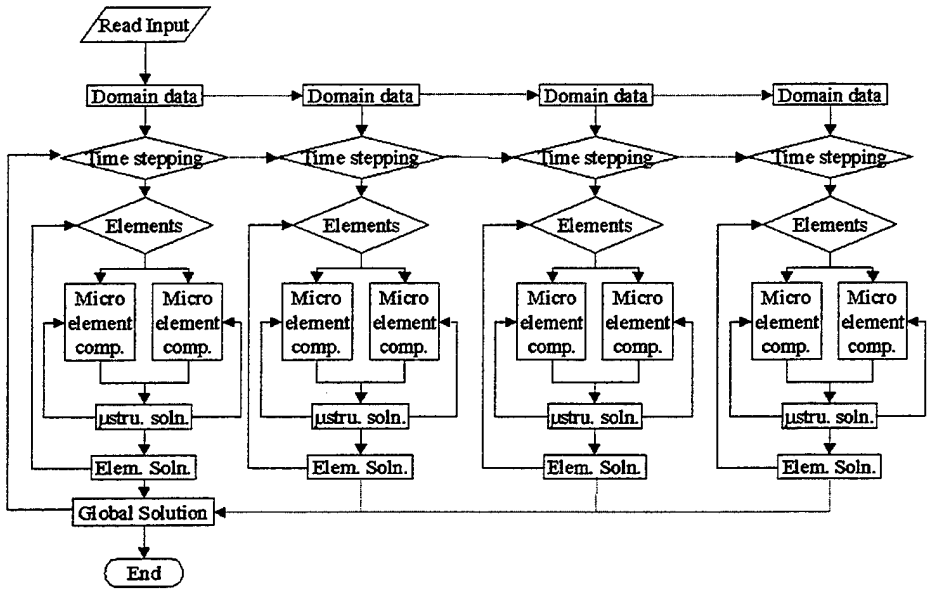

Figure 6. Program Flow for Strategy 2 With Helper Processors.

Computations in each micro-element involve updating the micro stresses, micro plastic strains, micro strain rates, and the micro mechanical and plastic properties. As shown in Figure 6, these computations are carried with the aid of helper processors in the second strategy. After this, the corresponding quantities are aggregated at the macro element level and mass and internal force vectors are computed for each macro element. In this manner after each macro element and its micro-elements are computed, the mass and internal force vectors are assembled across the macro elements in all the domains. After all the elements are computed, the mass and internal force information is exchanged for the nodes that are shared across the domain boundaries. The fully assembled mass and internal force vectors are later used for obtaining a new set of accelerations. After updating the velocities and geometry (and after checking for possible contacts and failures), the next time step is commenced. In each time step, the domain processor does these computations in serial manner first by calling the macro elements and then the micro-elements resident in each macro element.

The number of helper processors (n_h) that are needed, in the second strategy above, for each domain depends on several factors including the micro-structural model size, finite element interpolations, constitutive behavior of the material micro-components, and the complexity of the homogenization theory that is being used. Along with size and shape, the number of micro-elements determines the complexity. Thus, if one limits the type of micro-structures in a domain to just one kind, then the number of micro-elements (n_m) appearing in each macro-element would be constant; and then one can begin with a number of helper processors that equals to this number (i.e., $n_h = n_m$).

If n_h is set equal to n_m, however, the parent domain processor becomes idle while the micro-element computations are going on. To avoid this, n_h is set equal to $n_m - 1$, forcing the domain processor participate in doing one of the micro-element computations.

4. Scalability Studies

The results from the first strategy (i.e., with domain decomposition and no helper processors for micro-element computation) are presented in Table 1.

Table 1. Results for the Taylor Problem Without Helper Processors

Column 1	Column 2	Column 3	Column 4	Column 5
No. of Processors	Avg. Computation Time per Domain Processors, λ_{dc} (s)	Avg. Communication Time Between Domain Processors, λ_{dd} (s)	Avg. Wait Time per Domain Processors, λ_{dw} (s)	Run Time, λ_1 (s)
1	40,474	—	—	40,474
2	18,470	6	2,445	20,921
4	8,526	6	2,397	10,929
8	3,922	5	1,774	5,701
16	1,860	5	1,077	2,942
32	943	7	565	1,515
64	507	14	336	857

By the results in columns 2 and 5 in Table 1, one can conclude that the computation and overall run times are fairly scaled with the number of processors. This was achieved despite the fair amount of wait time that the processors had to endure. This wait time occurred as a result of having more elements in some processors becoming plastic and thus needing more micro-element computations than others.

This wait time can be reduced significantly by moving such elements evenly among all the processors. This was a result of the nature of the domain decomposition used on the input data set. With a prior knowledge of such deformation an even distribution of the plastic elements can be achieved. Even though such knowledge is available in the present Taylor impact problem,

elements were not redistributed because the results for the run time scaled fairly. In the present problem, there was an impact in the longitudinal direction causing a radial distribution of the plastic elements. In spite of this, a longitudinal decomposition was employed which meant that domains away from the impact had to wait until their elements become plastic.

The times of communication among the domain processors, as evident from the results in column 3 in Table 1, were fairly small. The results for the same problem with the second strategy of computation are presented in Table 2. In this strategy, helper processors were provided to help in the micro-element computations. Since the example problem had microstructures in all the global or macro elements, since each microstructure had two elements, and since the domain processors are also used in all the micro-element computations, one helper processor each was provided for each global domain processor. The results are presented in Table 2.

Table 2. Results for the Taylor Problem With Helper Processors

Column 1	Column 2	Column 3	Column 4	Column 5	Column 6	Column 7	Column 8	Column 9	Column 10
No. of domain processors	No. of helper processors	λ_{dd} (s)	λ_{dw} (s)	$\lambda_{dh\text{-}d}$ (s)	λ_{dc} (s)	$\lambda_{dh\text{-}h}$ (s)	λ_{hc} (s)	λ_{hw} (s)	λ_2 (s)
1									40,474
2	2	7	2,004	560	13,359	6,526	5,540	3,864	15,930
4	4	6	1,975	268	6,103	4,005	2,630	1,717	8,352
8	8	5	1,458	125	2,797	2,377	1,230	778	4,385
16	16	5	875	59	1,332	1,312	579	380	2,271
32	32	9	462	30	690	687	290	214	1,191

Note: λ_{dd} = Average time per domain processor for communication with domain processors.
λ_{dw} = Average time per domain processor waiting for end of computations in other domains.
$\lambda_{dh\text{-}d}$ = Average time per domain processor for communication with helper processors.
λ_{dc} = Average time per domain processor for computation, = $\lambda_2 - \lambda_{dd} - \lambda_{dw} - \lambda_{dh\text{-}d}$.
$\lambda_{dh\text{-}h}$ = Average time per helper processor for communication with domain processors.
λ_{hc} = Average time per helper processor for doing micro-element computations.
λ_{hw} = Average time per helper processor for waiting, = $\lambda_2 - \lambda_{hc} - \lambda_{dh\text{-}h}$.
λ_2 = Average wall clock run time per processor.

From the results shown in column 10 in Table 2, one can conclude that the overall run times are fairly scaled with the number of processors. The computation times logged by the domain and helper processors, columns 6 and 8, show that the micro-element computations consume a significant amount of time.

The practical benefit achieved by using the helper processors can be determined by considering the overall run times. When the wall clock run times in the last two columns of Tables 1 and 2 are considered solely in terms of the number of domain processors available (as shown in Figure 7), then the reductions in the wall clock run time are significant with the helper processors. However, when the same times are examined by considering that one could have used helper processors as domain processors, then it must be concluded that the helper processors are not utilized in an efficient manner. The run times with helper processors show an average increase of 35%, but such cursory examination is misleading because the wall clock run times included the wait times. These times are significant as shown for the domain processors in column 4 in Table 1 and column 4 in Table 2 and for the helper processors in column 9 in Table 2. Since these times can be eliminated with suitable input data set decomposition, the wall clock run times should be compared without these wait times. When this is done as shown in Table 3, the penalty reduces to an average of 9%. The results for the penalty are plotted against the total number of processors in Figure 8.

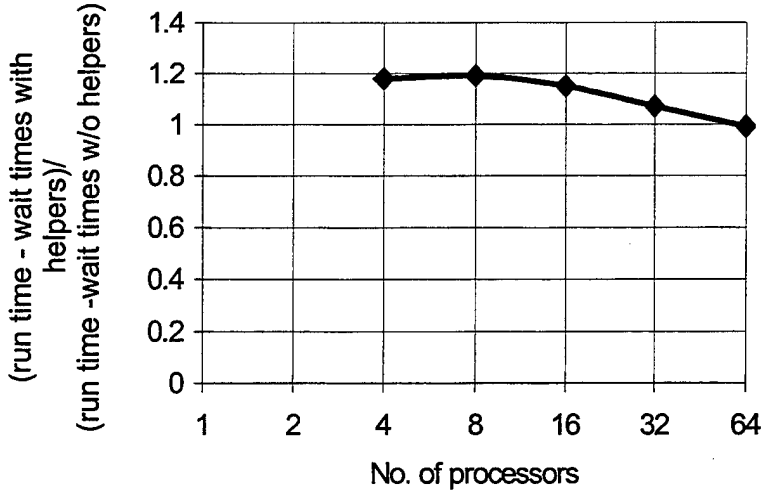

Figure 7. Total Run Times for the Two Strategies.

Table 3. Effective Run Times in the Two Strategies

No. of Total Processors	Strategy 2				Strategy 1			Penalty
	λ_{dw} (s)	λ_{hw} (s)	λ_2 (s)	Effective Run Time (s)	λ_{dw} (s)	λ_1 (s)	Effective Run Time (s)	
4	20,04	3,864	15,930	10,062	2,397	10,929	8,532	1.18
8	1,975	1,717	8,352	4,660	1,774	5,701	3,927	1.19
16	1,458	778	4,385	2,149	1,077	2,942	1,865	1.15
32	875	380	2,271	1,016	565	1,515	950	1.07
64	462	214	1,191	515	336	857	521	0.99

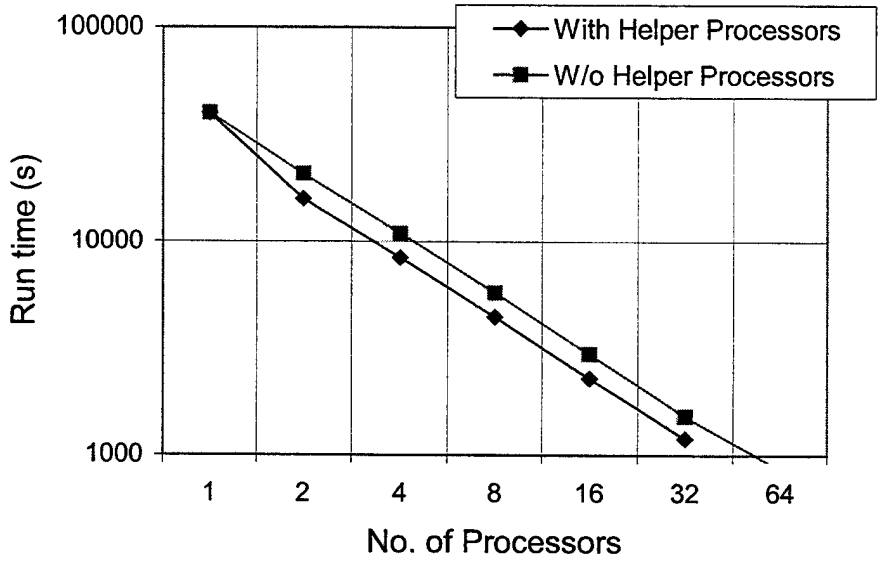

Figure 8. Total Run Times for the Two Strategies vs. Total Number of Processors.

In addition to the wait times, there is a potential for reducing the communication time between the domain and helper processors (i.e., the times shown in columns 5 and 7 of Table 2). The input to and the output from the micro-element computations were not minimized and packed with any due consideration. When this is done, the above penalty will reduce even further perhaps showing real gains for larger size microstructure idealizations. These and the results from the third strategy are in progress now.

5. Concluding Remarks

In this report, scalable implementation of nonlinear explicit AEH for solving coupled micro and macro structural applications is presented. Scalability of the approach is demonstrated for a standard Taylor's impact test problem. It provides some data for using the helper processors for micro-element computations in dual-level finite element modeling with embedded micro structural models. The following conclusions can be identified from the present study.

- Penalty, which is caused by the additional communication between domain and helper processors, reduces as the number of processors is increased.

- In any given time step, computations in some domains may finish ahead of other domains. Processors of these domains may be used to help out the still ongoing computations at other domains. In the example problem, a greater number of processors become available for computing the plastic elements if the number of domains is increased.

- The benefit of having additional processors for computation may outweigh the communication penalty as the size of the micro-structural model is increased.

- An understanding of micro-material model details to be communicated vs. micro material model computation is needed for material modelers.

INTENTIONALLY LEFT BLANK.

6. References

1. C. Licht, Frottement. "Viscoplasticité et Homogenization." Thesis, Université Montpellier, 1987.

2. Lene, F. "Contribution à Lètude des Matériaux Composites et de Leur Endommagement." Thesis, Université Paris, 1984.

3. Moulinec, M., and P. Suquet. "A Fast Numerical Method for Computing the Linear and Nonlinear Mechanical Properties of Composites." *C. R. Acad. Sci.*, Paris, pp. 1417–1423, 1994.

4. Benoussan, A., J. L. Lions, and G. Papanicolaou. *Asymptotic Analysis for Periodic Structures.* New York: North Holland Publishing Co., 1978.

5. Sanchez-Palencia, E. "Non-Homogeneous Media and Vibration Theory – Lecture Notes in Physics." Vol. 127, Springer Verlag, 1980.

6. Hashin, Z. "The Elastic Modulii of Heterogeneous Materials." *ASME Journal of Applied Mechanics*, vol. 29, pp. 143–150, 1962.

7. Hashin, Z., and S. Strickman. "A Variational Approach to the Theory of the Elastic Behavior of Multiphase Materials." *Journal of Mechanics and Physics of Solids*, vol. 11, pp. 127–140, 1963.

8. Hill, R. "Theory of Mechanical Properties of Fiber Toughened Materials." *Journal of Mechanics and Physics of Solids*, vol. 12, pp. 199–212, 1964.

9. Willis, J. *Elastic Theory of Composites, in: Mechanics of Solids.* Oxford: Pergamon Press, pp. 353–386, 1982.

10. Suquet, F. "Plasticité et Homogenization." Thesis, Université Paris, 1982.

11. Fish, J., K. Shek, M. Pandheeradi, and M. Shepard. "Computational Plasticity for Composite Structures Based on Mathematical Homogenization: Theory and Practice." *Computer Methods in Applied Mechanics and Engineering*, vol. 148, nos. 1–2, pp. 53–73, 1997.

12. Terada, K., and N. Kikuchi. "Nonlinear Homogenization Method for Practical Applications." *Computational Methods in Micro-mechanics*, American Society of Mechanical Engineers, Applied Mechanics Division, AMD, vol. 212, pp. 1–16, 1995.

13. Ghosh, S., and S. Moorthy. "Elasto-plastic Analysis of Arbitrary Heterogeneous Materials With the Voronoi Cell Finite Element Method." *Computer Method in Applied Mechanics and Engineering*, vol. 121, pp. 373–409, 1995.

14. Lene, F. "Damage Constitutive Relations for Composite Materials." *Engineering Fracture Mechanics*, vol. 25, nos. 5–6, pp. 713–728, 1986.

15. Guedes, J. M., and N. Nikuchi. "Preprocessing and Post-processing for Materials Based on the Homogenization Method With Adaptive Finite Element Methods." *Computer Methods in Applied Mechanics and Engineering*, vol. 83, no. 2, pp. 143–198, October 1990.

16. Chung, P. W., R. R. Namburu, and K. K. Tamma. "Three-Dimensional Elasto-plastic Heterogeneous Media Subjected to Short Transient Loads." AIAA paper-99-1239, 1999.

17. Hoover, G. G., A. J. DeGroot, J. D. Maltby, and R. J. Procassini. *PARADYN – DYNA3D for Massively Parallel Computers.* UCRL 53868-94, Engineering Research, Development and Technology FY94, Lawrence Livermore National Laboratory, Livermore, CA, 1995.

18. Plimpton, S., S. Attaway, B. Hendrickson, J. Sweagle, C. Vaughan, and D. Gardner. "Transient Dynamic Simulations: Parallel Algorithms for Contact Detection and Smoothed Particle Hydrodynamics." Proceedings of SuperComputing 96, Pittsburgh, PA, 1996.

19. Namburu, R. R. "Unified Finite Element Methodology for Thermal-Structural Problems." Ph. D. thesis, University of Minnesota, July 1991.

20. Tamma, K. K., and R. R. Namburu. "A Robust Self Starting Explicit Computational Methodology for Structural Dynamic Applications: Architecture and Representations." *International Journal for Numerical Methods in Engineering*, vol. 29, pp. 1441–1454, 1990.

21. Karypis, G., and V. Kumar. "A Fast and High Quality Multilevel Scheme for Partitioning Irregular Graphs." TR 95-035, Department of Computer Science, University of Minnesota, 1995.

Glossary

Unless stated otherwise, all indices vary according to dimensionality of the problem (e.g., i = 1, 2, 3 in a three-dimensional structure).

$\bar{\varepsilon}^p$	effective plastic strain
χ_i^{jk}	a corrector
$\chi_i^{jk^1}$	first elasto-plastic corrector
$\chi_i^{jk^2}$	second elasto-plastic corrector
$[\,]$	matrix quantity
$[\,]^T$	matrix transpose
$\{\}$	vector quantity
C_{ijkl}	a fourth order material property tensor
D	a fluidity parameter
e_{ij}	a strain vector
F_1	summed internal pre-stress force vector
F_2	summed external force vector
F_3	summed body force vector
f_i	a body force vector
G	shear modulus
H'	a hardening parameter
K	bulk modulus
M, M_{ij}	mass matrix
n_h	number of helper processors
n_i	a normal vector
n_m	number of micro-elements in a macro-element
P	pressure
p	a fluidity parameter
Q_{ij}	a normal vector to the yield surface
R	rate dependent radius of the yield surface
S_{ij}	a deviatoric stress tensor
sub-subscript n	used for u_i, v_i, σ_i, and e_i to denote Y-periodic functions
superscript ε	micro/macro continuum solutions
superscript J	Jaumann definition of a co-rotated quantity
superscript n	values at the nth time step
t	time
T_i	a surface traction vector
u_i	a displacement vector
v_i	a velocity vector
x_i	a position vector
y_i	a position vector

$\Delta\lambda$	a scalar quantity representing the magnitude of the radial return correction
$\dot{}$	a time derivative
E	an internal energy
Γ_1	surface of a boundary on which displacement conditions are prescribed
Γ_2	surface of a boundary on which traction conditions are prescribed
Ω	a domain
δ_{ij}	Kronecker delta
ε	a small positive number
ϕ	a Y-periodic function
γ	a scalar quantity used in the time integration
λ_1	run time with only domain decomposition and no helper processors
λ_2	run time with only domain decomposition and helper processors
λ_{dc}	average computation time on domain processors
λ_{dd}	average communication time between domain processors
$\lambda_{dh\text{-}d}$	average time for domain processors for communication with helper processors
$\lambda_{dh\text{-}h}$	average time for helper processors for communication with domain processors
λ_{dw}	average wait time on domain processors
λ_{hc}	average computation time on helper processors
λ_{hw}	average wait time on helper processors
ρ	density
σ_i	a stress tensor
σ_Y^0	static yield stress
ω_{kj}	a rotational vector

NO. OF COPIES	ORGANIZATION
2	DEFENSE TECHNICAL INFORMATION CENTER DTIC OCA 8725 JOHN J KINGMAN RD STE 0944 FT BELVOIR VA 22060-6218
1	HQDA DAMO FDT 400 ARMY PENTAGON WASHINGTON DC 20310-0460
1	OSD OUSD(A&T)/ODDR&E(R) DR R J TREW 3800 DEFENSE PENTAGON WASHINGTON DC 20301-3800
1	COMMANDING GENERAL US ARMY MATERIEL CMD AMCRDA TF 5001 EISENHOWER AVE ALEXANDRIA VA 22333-0001
1	INST FOR ADVNCD TCHNLGY THE UNIV OF TEXAS AT AUSTIN 3925 W BRAKER LN STE 400 AUSTIN TX 78759-5316
1	DARPA SPECIAL PROJECTS OFFICE J CARLINI 3701 N FAIRFAX DR ARLINGTON VA 22203-1714
1	US MILITARY ACADEMY MATH SCI CTR EXCELLENCE MADN MATH MAJ HUBER THAYER HALL WEST POINT NY 10996-1786
1	DIRECTOR US ARMY RESEARCH LAB AMSRL D DR D SMITH 2800 POWDER MILL RD ADELPHI MD 20783-1197

NO. OF COPIES	ORGANIZATION
1	DIRECTOR US ARMY RESEARCH LAB AMSRL CI AI R 2800 POWDER MILL RD ADELPHI MD 20783-1197
3	DIRECTOR US ARMY RESEARCH LAB AMSRL CI LL 2800 POWDER MILL RD ADELPHI MD 20783-1197
3	DIRECTOR US ARMY RESEARCH LAB AMSRL CI IS T 2800 POWDER MILL RD ADELPHI MD 20783-1197
	ABERDEEN PROVING GROUND
2	DIR USARL AMSRL CI LP (BLDG 305)

NO. OF COPIES	ORGANIZATION
1	DIRECTOR US ARMY RESEARCH LAB AMSRL CP CA D SNIDER 2800 POWDER MILL RD ADELPHI MD 20783-1145
1	DIRECTOR US ARMY RESEARCH LAB AMSRL OP SD TA 2800 POWDER MILL RD ADELPHI MD 20783-1145
1	DIRECTOR DA OASARDA SARD SO 103 ARMY PENTAGON WASHINGTON DC 20310-0103
1	DEPUTY ASST SCY FOR R&T SARD TT RM 3EA79 THE PENTAGON WASHINGTON DC 20301-7100
1	COMMANDER US ARMY TACOM PM TACTICAL VEHICLES PM RDT&E 6501 ELEVEN MILE ROAD WARREN MI 48397-5000
3	COMMANDER US ARMY TACOM PM TACTICAL VEHICLES SFAE TVL SFAE TVM SFAE TVH 6501 ELEVEN MILE RD WARREN MI 48397-5000
1	COMMANDER US ARMY TACOM PM TACTICAL SURVIVABLE SYSTEMS SFAE GCSS W GSI H 6501 ELEVEN MILE RD WARREN MI 48397-5000

NO. OF COPIES	ORGANIZATION
7	COMMANDER US ARMY TACOM ASMTA TR R J CHAPIN R MCCLELLAND J FLORENCE J THOMSON K BISHNOI 6501 ELEVEN MILE RD WARREN MI 48397-5000
3	DIRECTOR US ARMY RESEARCH LAB AMSRL OP SD TL 2800 POWDER MILL ROAD ADELPHI MD 20783-1145
	ABERDEEN PROVING GROUND
1	DIR USARL AMSRL CI H C NIETUBICZ

REPORT DOCUMENTATION PAGE

Form Approved
OMB No. 0704-0188

1. AGENCY USE ONLY *(Leave blank)*	2. REPORT DATE	3. REPORT TYPE AND DATES COVERED
	September 2000	Final, October–September 1999

4. TITLE AND SUBTITLE
Scalable Implementation of Three-Dimensional Heterogeneous Media Subjected to Short Transient Impact Loads

5. FUNDING NUMBERS
61102H48
665803.731

6. AUTHOR(S)
Rama R. Valisetty, Raju R. Namburu, and Peter W. Chung

7. PERFORMING ORGANIZATION NAME(S) AND ADDRESS(ES)
U.S. Army Research Laboratory
ATTN: AMSRL-CI-HC
Aberdeen Proving Ground, MD 21005-5067

8. PERFORMING ORGANIZATION REPORT NUMBER
ARL-TR-2351

9. SPONSORING/MONITORING AGENCY NAMES(S) AND ADDRESS(ES)

10.SPONSORING/MONITORING AGENCY REPORT NUMBER

11. SUPPLEMENTARY NOTES

12a. DISTRIBUTION/AVAILABILITY STATEMENT
Approved for public release; distribution is unlimited.

12b. DISTRIBUTION CODE

13. ABSTRACT *(Maximum 200 words)*

This report is concerned with developing and implementing scalable algorithmic approaches for solving coupled micro and macro structural applications based on the asymptotic expansion homogenization (AEH) method. AEH for nonlinear and short transient loading applications is computationally demanding and cannot be addressed on serial computers. Hence, the emphasis of the present investigation is to develop and implement consistent AEH numerical formulations on scalable computers to address elasto-plastic material response of structures subjected to short transient loading. A second order, accurate velocity-based, explicit time integration method, in conjunction with the AEH method on scalable computing architectures, is implemented using message passing interface (MPI). Two different scalable implementation approaches are discussed, and the scalability of the computational approach is demonstrated.

14. SUBJECT TERMS
parallel computing, scalable computing, domain decomposition, micro-mechanics

15. NUMBER OF PAGES
36

16. PRICE CODE

17. SECURITY CLASSIFICATION OF REPORT	18. SECURITY CLASSIFICATION OF THIS PAGE	19. SECURITY CLASSIFICATION OF ABSTRACT	20. LIMITATION OF ABSTRACT
UNCLASSIFIED	UNCLASSIFIED	UNCLASSIFIED	UL

INTENTIONALLY LEFT BLANK.

USER EVALUATION SHEET/CHANGE OF ADDRESS

This Laboratory undertakes a continuing effort to improve the quality of the reports it publishes. Your comments/answers to the items/questions below will aid us in our efforts.

1. ARL Report Number/Author ARL-TR-2351 (Valisetty) Date of Report September 2000

2. Date Report Received _____

3. Does this report satisfy a need? (Comment on purpose, related project, or other area of interest for which the report will be used.) _____

4. Specifically, how is the report being used? (Information source, design data, procedure, source of ideas, etc.) _____

5. Has the information in this report led to any quantitative savings as far as man-hours or dollars saved, operating costs avoided, or efficiencies achieved, etc? If so, please elaborate. _____

6. General Comments. What do you think should be changed to improve future reports? (Indicate changes to organization, technical content, format, etc.) _____

CURRENT ADDRESS

Organization

Name E-mail Name

Street or P.O. Box No.

City, State, Zip Code

7. If indicating a Change of Address or Address Correction, please provide the Current or Correct address above and the Old or Incorrect address below.

OLD ADDRESS

Organization

Name

Street or P.O. Box No.

City, State, Zip Code

(Remove this sheet, fold as indicated, tape closed, and mail.)

(DO NOT STAPLE)

DEPARTMENT OF THE ARMY

OFFICIAL BUSINESS

NO POSTAGE
NECESSARY
IF MAILED
IN THE
UNITED STATES

BUSINESS REPLY MAIL
FIRST CLASS PERMIT NO 0001,APG,MD

POSTAGE WILL BE PAID BY ADDRESSEE

DIRECTOR
US ARMY RESEARCH LABORATORY
ATTN AMSRL CI HC
ABERDEEN PROVING GROUND MD 21005-5067